

## Supporting Information

### **Constructing dual interfacial gold nanodot interlayers in sandwich-structured BaTiO<sub>3</sub>/P(VDF-HFP) composites for high energy storage density**

Peng Yin<sup>a</sup>, Xiaohan Bie<sup>a</sup>, Qingyang Tang<sup>a</sup>, Linwei Zhu<sup>a</sup>, Runhua Fan<sup>c</sup>, Davoud Dastan<sup>d</sup>, Hongzhi Cui<sup>a</sup>, Kun Zhang<sup>b, \*</sup>, Zhicheng Shi<sup>a, \*</sup>

<sup>a</sup>School of Materials Science and Engineering, Ocean University of China, Qingdao 266100, China.

<sup>b</sup>Key Laboratory of Microgravity (National Microgravity Laboratory), Institute of Mechanics, Chinese Academy of Sciences, Beijing 100190, China.

<sup>c</sup>College of Ocean Science and Engineering, Shanghai Maritime University, Shanghai 201306, China.

<sup>d</sup>Department of Materials Science and Engineering, Cornell University, Ithaca, NY, 14850, USA.

\*Corresponding author.

E-mail: zhangkun@imech.ac.cn (Kun Zhang); zcshi@ouc.edu.cn (Zhicheng Shi)

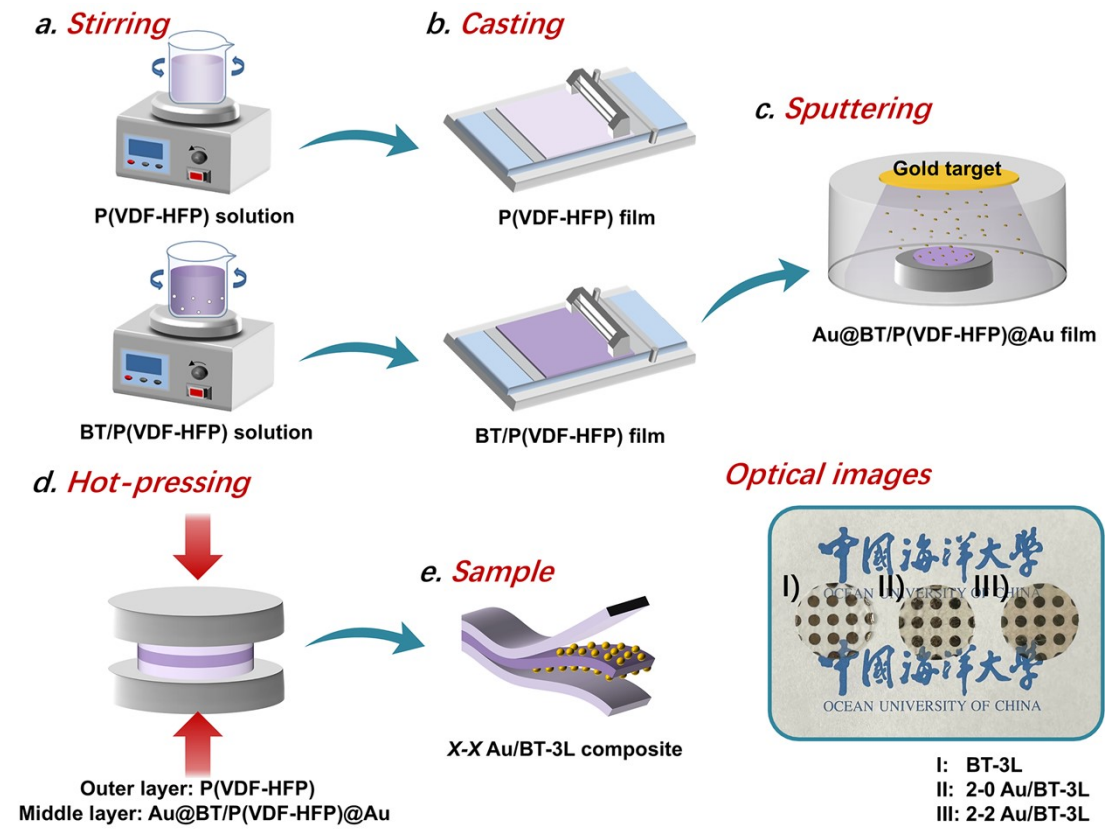


**Fig. S1** Preparation process flow of P(VDF-HFP) film, BT/P(VDF-HFP) film and  $x$ - $x$  Au/BT-3L composite (Inset: optical images of BT-3L, 2-0 Au/BT-3L and 2-2 Au/BT-3L composites).

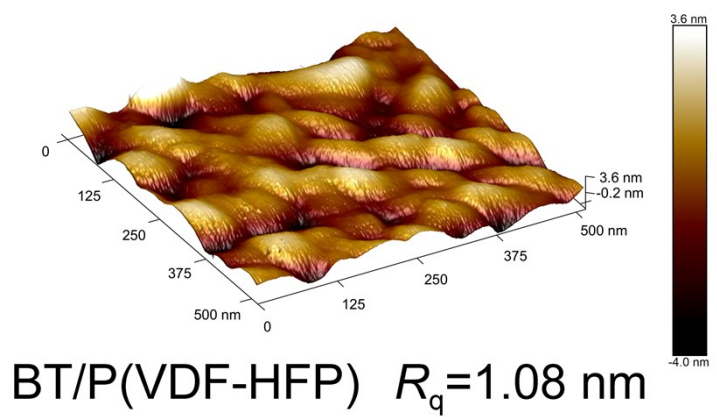


**Fig. S2** The 3D AFM morphology and surface roughness of BT/P(VDF-HFP) film.

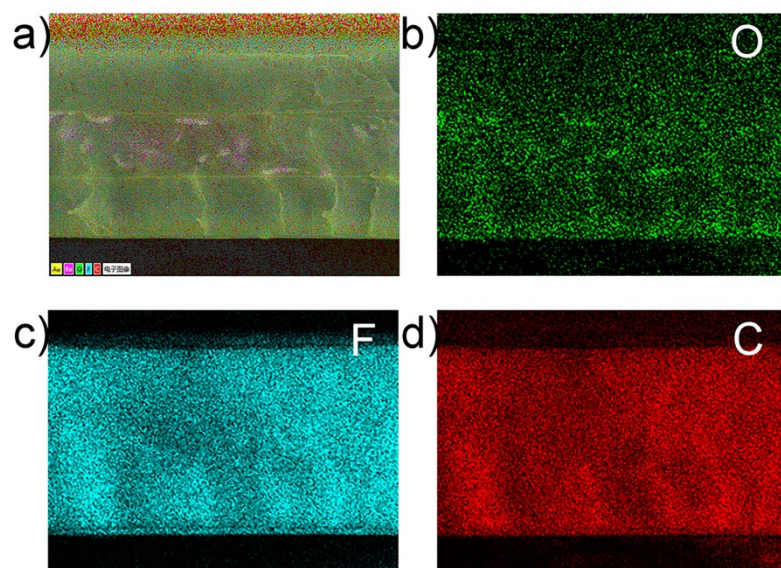


**Fig. S3** EDS mapping of O, F and C elements corresponds to 2-2 Au/BT-3L trilayer composite.

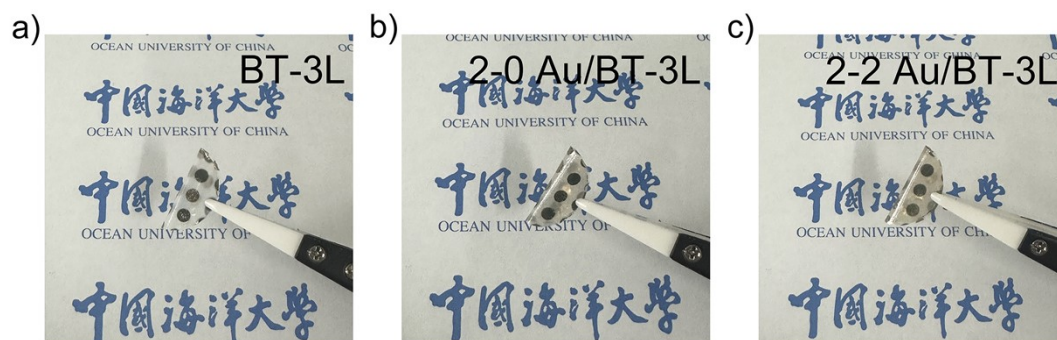


**Fig. S4** The optical images of flexibility validation of BT-3L, 2-0 Au/BT-3L and 2-2 Au BT/3L composites.

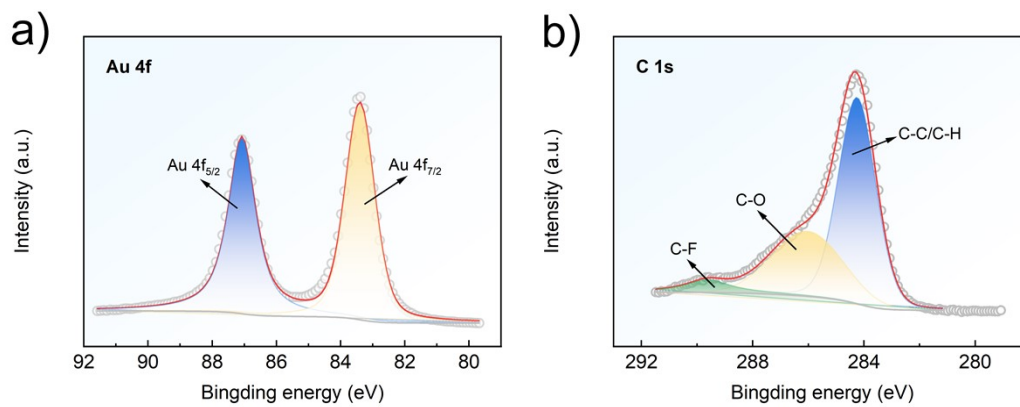


**Fig. S5** The XPS high-resolution spectra of (a) Au 4f and (b) C 1s for BT/P(VDF-HFP) film deposited with Au nanodots at sputtering time of 2 min.

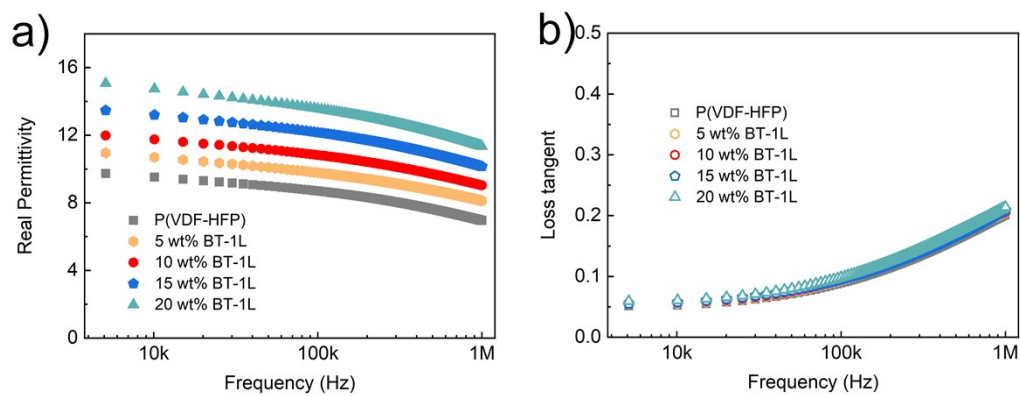


**Fig. S6** (a) Dielectric constant and (b) loss of BT-1L composites.

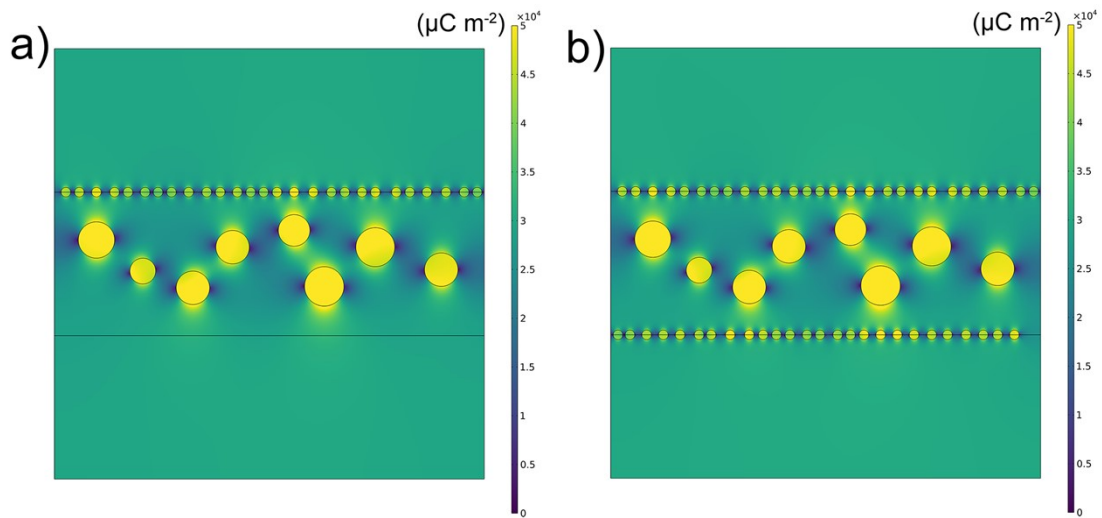


**Fig. S7** The simulated polarization distribution of (a)  $x=0$  Au/BT-3L and (b)  $x-x$  Au/BT-3L composites.

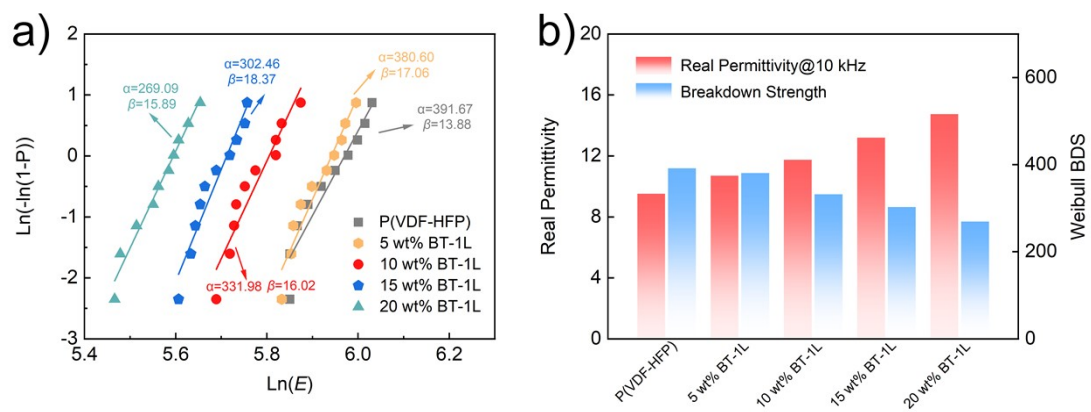


**Fig. S8** (a) Weibull distribution plots of BT-1L composites. (b) Comparison of dielectric and breakdown properties of BT-1L composites.

**Table S1** The summarized breakdown strengths ( $E_b$ ) in this work.

<b>Sample</b>	<b>Weibull <math>E_b</math> (MV m<sup>-1</sup>)</b>	<b>Shape Factor (<math>\beta</math>)</b>
P(VDF-HFP)	391.67	13.88
5 wt% BT/1L	380.60	17.06
10 wt% BT/1L	331.98	16.02
15 wt% BT/1L	302.46	18.37
20 wt% BT/1L	269.09	15.89
BT-3L	416.67	18.18
1-0 Au/BT-3L	465.38	20.86
2-0 Au/BT-3L	498.37	21.96
3-0 Au/BT-3L	448.11	18.53
4-0 Au/BT-3L	407.72	19.63
1-1 Au/BT-3L	501.24	20.43
2-2 Au/BT-3L	520.08	23.84
3-3 Au/BT-3L	469.07	22.54
4-4 Au/BT-3L	415.09	22.97

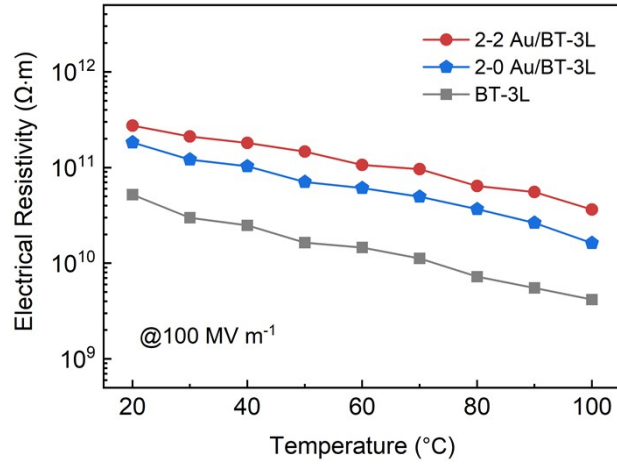


**Fig. S9** The temperature dependent resistivity of BT-3L, 2-0 Au/BT-3L and 2-2 Au/BT-3L composites, respectively.

**Table S2** The calculated results according to Equation (8) when  $d = 5 \mu\text{m}$ .

Radius of Au QDs	1 nm	1.5 nm	2 nm	2.5 nm	3 nm	4 nm
Capacitance $C$ ( $\times 10^{-18}$ F)	1.0588	1.5884	2.1179	2.6475	3.1772	4.2367
$e^2/2C$ ( $\times 10^{-20}$ J)	1.2089	0.8059	0.6044	0.4835	0.4029	0.3021
$T$ (K)	875.57	583.69	437.74	350.18	291.80	218.83

**Note:** Here,  $e \approx 1.6 \times 10^{-19}$  is electron charge,  $k_B \approx 1.380649 \times 10^{-23}$  J K<sup>-1</sup> is Boltzmann constant,  $\epsilon_0 = 8.85 \times 10^{-12}$  F m<sup>-1</sup> is vacuum permittivity,  $\epsilon_r$  is relative permittivity of P(VDF-HFP) matrix.

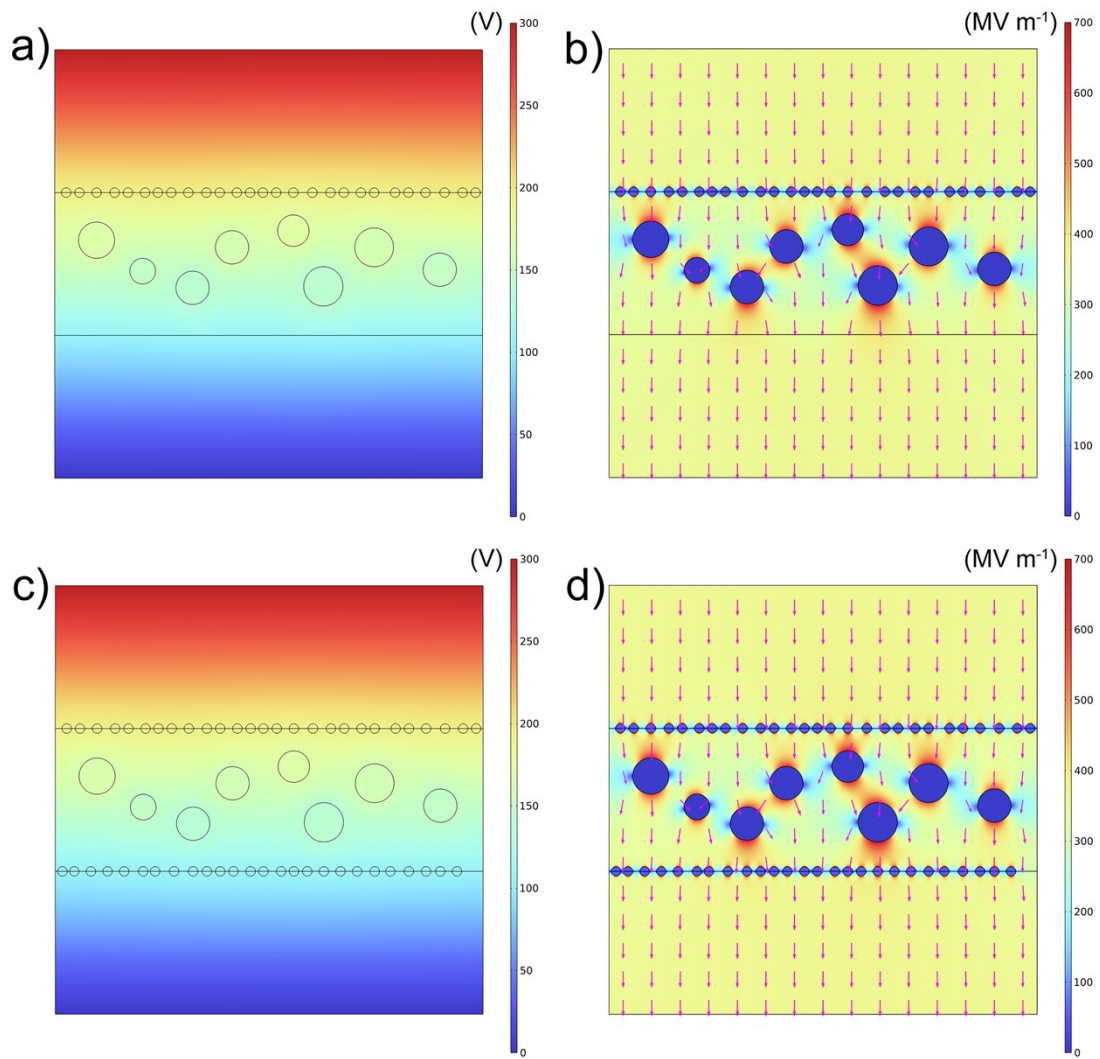


**Fig. S10** The simulation of electric potential and electric field distribution of (a, b)  $x-0$  Au/BT-3L composites and (c, d)  $x-x$  Au/BT-3L composites.



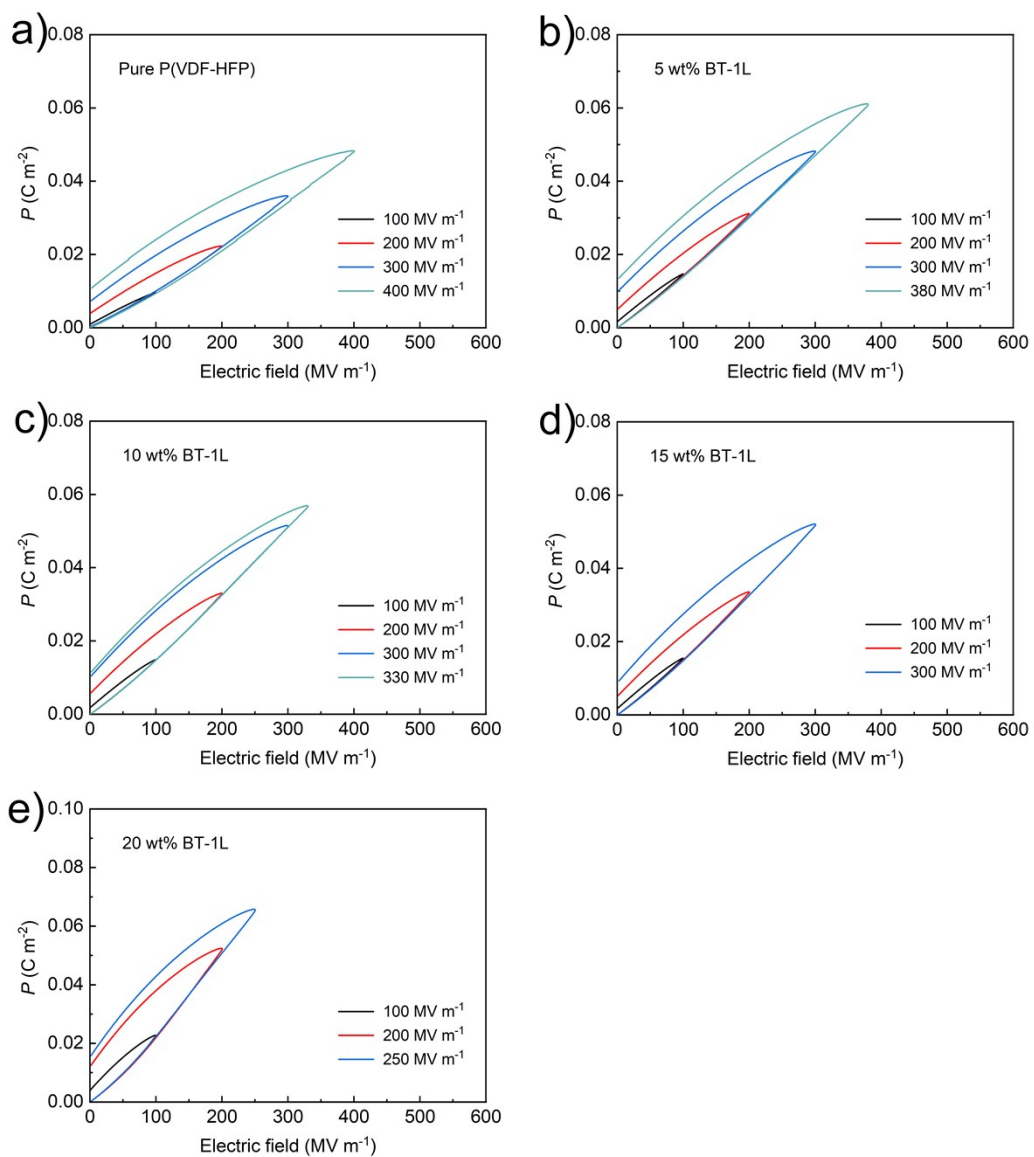


**Fig. S11** The  $D-E$  loops of (a) pure P(VDF-HFP) and (b–e) BT-1L composites.

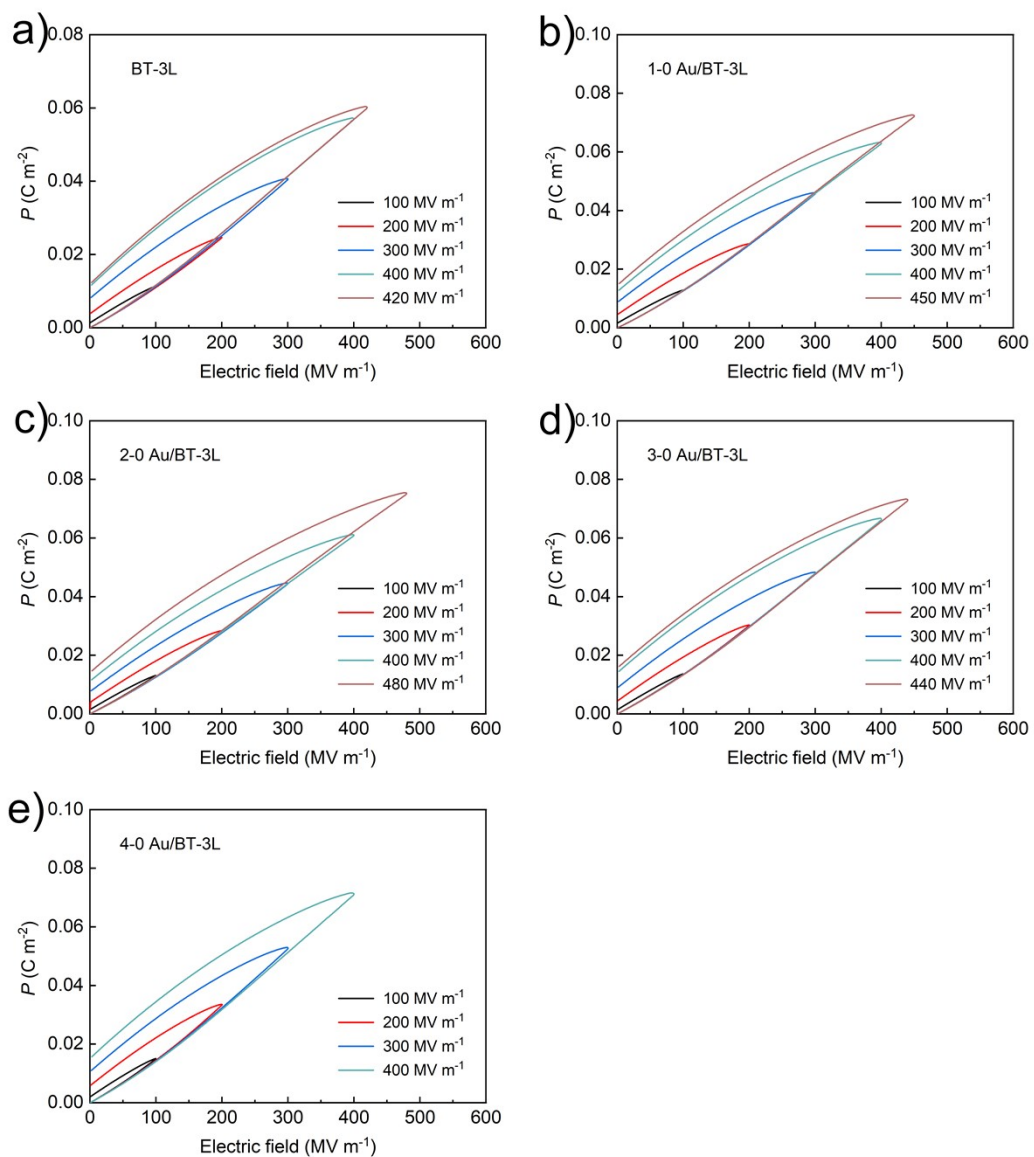


**Fig. S12** The  $D-E$  loops of (a) BT-3L composite and (b-e)  $x-0$  Au/BT-3L composites.

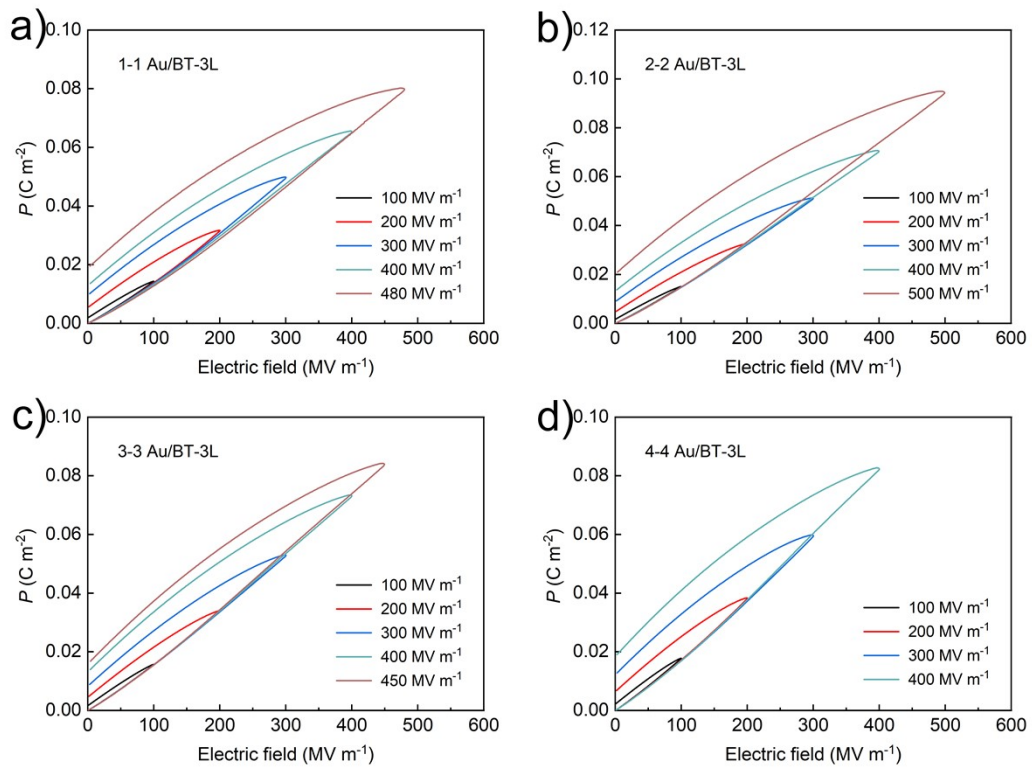


**Fig. S13** (a–d) The  $D$ – $E$  loops of  $x$ - $x$  Au/BT-3L composites.

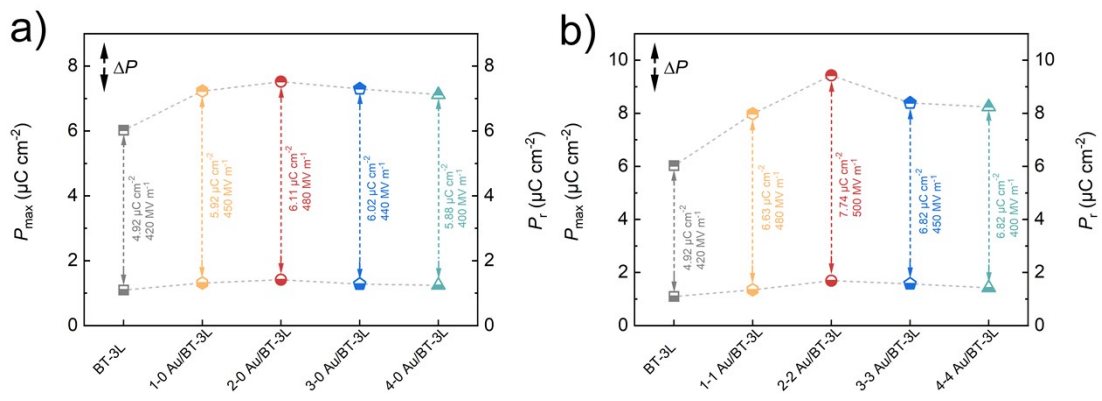


**Fig. S14** The maximum polarization difference ( $\Delta P$ ) of (a)  $x$ -0 Au/BT-3L composites and (b)  $x$ - $x$  Au/BT-3L composites.

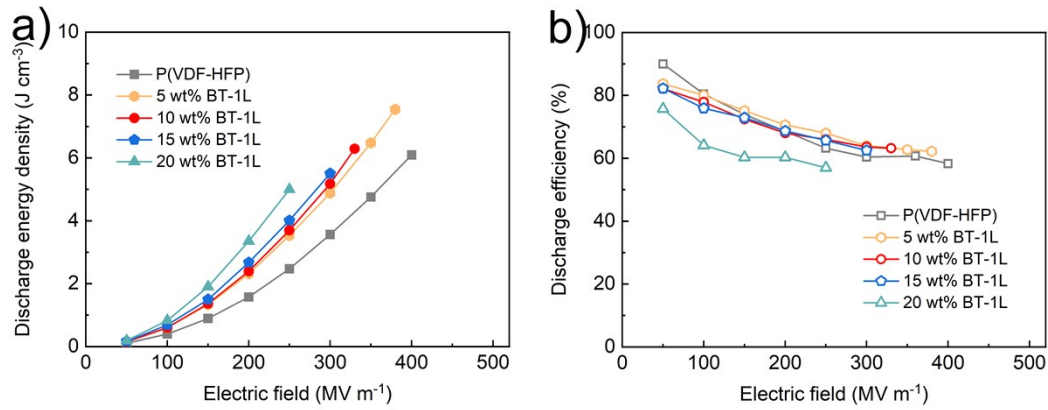


**Fig. S15** (a) The discharge energy density ( $U_d$ ) and (b) discharge efficiency ( $\eta$ ) of pure P(VDF-HFP) and BT-1L composites.

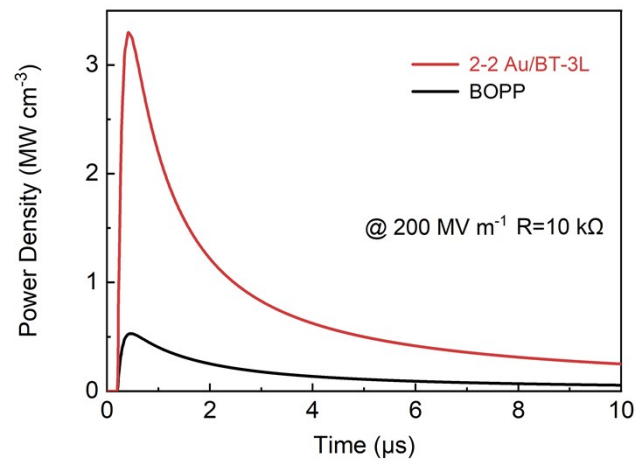


**Fig. S16** The power density as a function of discharge time of 2-2 Au/BT-3L composite and BOPP.

The applied electric field was 200 MV m<sup>-1</sup> and the loaded resistor was 10 kΩ.

The discharge energy density ( $W_d$ ) can be calculated using the equation:

$$W_d = \frac{\int U^2(t)dt}{RV} \# \quad (S1)$$

where  $U$ ,  $t$ ,  $R$  and  $V$  represent the discharge voltage, discharge time, load resistance and the volume of dielectrics, respectively.

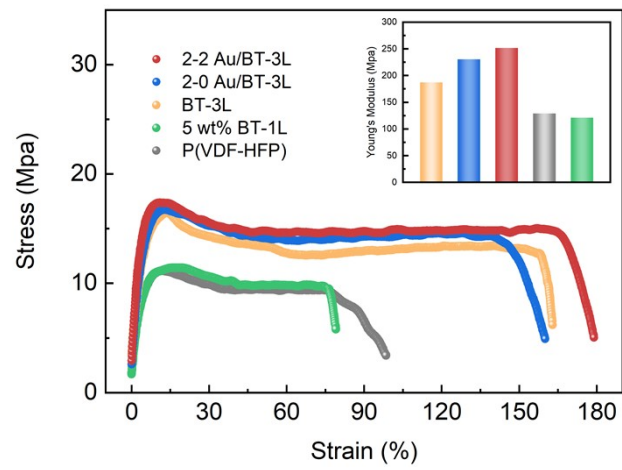


**Fig. S17** The stress-strain curves of P(VDF-HFP), 5 wt% BT-1L, BT-3L, 2-0 Au/BT-3L and 2-2 Au/BT-3L composites. Inset: Young's modulus of these composites.